This is the preprint of the article that appeared in final form in **Microelectronics Reliability** 102 : (2019) // Article ID 113500, which has been published in final form at https://doi.org/10.1016/j.microrel.2019.113500.

A methodology to determine reliability issues in automotive SiC power modules combining 1D and 3D thermal simulations under driving cycle profiles

A. Matallana[a,*], E. Robles[a], E. Ibarra[a], J. Andreu[a], N. Delmonte[b], P. Cova[b]

[a] *University of the Basque Country (UPV/EHU), Departamento Tecnología Electrónica, Plaza Ingeniero Torres Quevedo 1, 48013 Bilbao, Spain*
[b] *University of Parma (UNIPR), Dipartimento di Ingegneria e Architettura, Parco Area delle Scienze 181/A, 43124 Parma, Italy*

Abstract

Current environmental concerns and fuel scarcity are leading to the progressive introduction of Electric Vehicles (EV) in the global fleet vehicle population. This requires significant design and research efforts from scientific community and industry to provide reliable automotive electric propulsion systems. The power modules used for automotive traction inverters can be considered as central elements of such systems. As they are subject to high electro-thermal stress during operation, Design-for-Reliability (DfR) approaches should be adopted. Thus, accurate models for electro-thermal simulations are relevant since the early design stages. However, such simulations become highly time consuming and complex when accurate thermal characterization through standardized or real driving conditions needs to be provided. In this context, this work proposes a simulation methodology that combines real-time simulation for electro-thermal characterization of the whole EV propulsion system, using a 1D equivalent thermal impedance circuit, in conjunction with 3D FEM thermal simulation. In this way, an accurate thermal characterization of the power module under driving cycles with long duration (of hundreds of seconds) can be obtained without computing heavy 3D FEM simulations. The proposed procedure allows to simplify and speed up the early design stages while maintaining high accuracy in the results.

Keywords: Power electronics, EV, automotive power modules, Design-for-Reliability, FEM, real-time simulation, electro-thermal simulation, driving cycle

1. Introduction

Due to current environmental concerns such as pollution and climate change, Electric Vehicles (EV) are being considered as an alternative to conventional Internal Combustion Engine (ICE) based vehicles [1, 2]. The main technologies that must be developed in order to make the EV technology a competitive transport solution are the battery packs [3], electric machines [4, 5], power electronics [6, 7], electronic control units (ECU) [8] with their corresponding control algorithms [9], and the cooling systems [10, 11].

The power system can be considered as the core element of the EV powertrain, as it is responsible of transferring a significant amount of energy from the battery to the electric machine during motoring operation, and from the machine to the battery during regenerative braking. The two-level three-phase inverter is the most common automotive propulsive power conversion topology where, in general, two approaches are followed to implement the power switches of an automotive converter [7]: (a) discrete semiconductor devices (Tesla) and (b) power modules in half-bridge or six-pack configuration with single sided (Nissan, BMW, Audi) or double side (Toyota, Chevrolet) cooling. Thus, it can be said that the major manufacturers rely on power module technology. All these industrial solutions are based on silicon IGBTs. However, a gradual transition to silicon carbide (SiC) technologies can be expected for next generation automotive power converters [12–14].

Regardless of power semiconductor technology, a power module is a multilayer structure consisting of various materials (silicon, copper, ceramic materials, etc.), each with its particular Coefficient of Thermal Expansion (CTE) [15]. During thermal or power cycling, these CTE mismatches produce thermo-mechanical fatigue, introducing possible mechanical failures over time and compromising the long term reliability of such critical elements [16]. This issue is specially relevant in both solder layers and interconnection components (i.e, bond wires) [17]. In this scenario, electro-thermal simulation can be considered a powerful tool to analyse, determine hot spots, (re)design and determine life-cycles of automotive power modules during early development stages [16, 18–21] following a DfR approach [16]. In this way, design errors and reliability problems can be found and solved before the expensive prototyping stage, accelerating the whole R&D process and meeting the life-cycle requirements of the automotive industry (i.e., about 10 to 15 years of failure-free operation [16]).

When performing electro-thermal simulations of an EV power module within a complete drive system, it is of great in-

*Corresponding author
Email addresses: asier.matallana@ehu.eus, Tel. +0034 94 601 72 43 (A. Matallana), endika.robles@ehu.eus (E. Robles), edorta.ibarra@ehu.eus (E. Ibarra), jon.andreu@ehu.eus (J. Andreu), nicola.delmonte@unipr.it (N. Delmonte), paolo.cova@unipr.it (P. Cova)

terest to study its dynamic performance (electrical and thermal) under real or standardized driving conditions [22], as this will provide valuable information regarding system performance, reliability and life-cycle estimation [21]. In this context, a number of standardized driving cycles have been proposed in the last decades to evaluate the system behaviour under real operation conditions. For example, the New European Driving Cycle (NEDC) [23] has been used in Europe, although it is being substituted by the Worldwide Harmonized Light-Duty Vehicles Test Procedure (WLTP) [24]. Such cycles are suitable for gasoline and diesel vehicles; however, various specific cycles are being defined in order to characterize the driving conditions of EVs, as the way of driving such vehicles is heavily conditioned by the range anxiety phenomena [25].

Finite Element Method (FEM) simulation is commonly used for the realization of accurate 3D electro-thermal simulations [26, 27], allowing full layout characterization (Table 1). However, there are significantly different time-constants involved in the model (ranging from microseconds to characterize the electric machine, power system behaviour and instantaneous power losses, to hundreds of seconds to characterize the vehicular model and the driving cycle itself), and also various physics to be simulated; thus, the complexity and computational burden becomes excessive to exclusively rely on 3D FEM for long driving cycle simulation [28, 29]. On the other hand, simplified thermal simulation approaches based on equivalent 1D Foster and Cauer (RC) networks [20, 30] can be conducted, as the computational burden is significantly lower (Table 1). However, if only this simulation method is used, the designer is not able to characterize the thermal distribution of the whole power module.

In order to simplify, speed up the whole electro-thermal simulation stage and achieve highly accurate and representative full layout results, a complete methodology that combines the usage of 3D FEM, simplified 1D modelling and real-time (RT) simulation is proposed in this paper. In this way, the accuracy of physical simulation (for power module thermal characterization) and fastness of real-time simulation (for vehicular and drive system simulation) are mixed, obtaining the best features of both worlds. In order to show the benefits of the proposal, such methodology has been implemented during the electro-thermal simulation stage of a SiC based half-bridge power module (composed by four SiC MOSFETs with their corresponding anti-parallel freewheeling SiC JBS diodes). In particular, COMSOL Multiphysics software has been used to solve 3D thermal FEM simulations, while an OPAL-RT OP4510 digital platform has been used to conduct real-time simulations with 1D thermal characterization over the standardized driving cycles. The obtained results show the convenience of the proposed work-flow, as accuracy for thermal characterization is guaranteed while reducing the time required to carry out all the simulations.

In the following, the work-flow of the proposed modelling and simulation procedure and its associated tools are described.

Table 1: Qualitative comparison between 3D FEM, 1D Cauer/Foster and the proposed hybrid simulation procedures.

Features	3D FEM	1D Cauer/Foster	Proposed hybrid methodology
Computational load	✗	✓✓	✓
Simulation complexity	✗	✓✓	✓
Integration of thermal properties(1)	✓✓	✗	✓✓
Integration of electrical properties(2)	✗	✓	✓
Number of evaluation points(3)	✓✓✓	✗	✓✓✓

(1) The 3D FEM uses thermal physics, the 1D procedure uses equivalent Cauer/Foster networks (simplification and loss of information).
(2) The 3D FEM uses electrical physics, the 1D Cauer/Foster procedure uses the power semiconductor loss models.
(3) The 3D FEM evaluates the complete layout, while the 1D Cauer/Foster procedure only evaluates only some points of it.

2. Proposed hybrid 1D/3D electro-thermal modelling and simulation procedure

Figure 1 shows the general diagram of the proposed hybrid 1D/3D electro-thermal simulation procedure. The block of the left hand of Figure 1 (in blue) represents the steps to be carried out by 1D RT simulation, while the block of the right hand (in green) shows the steps to be carried out using 3D FEM analysis. Between both blocks, a number of steps that must be carried out in order to process data from 1D to 3D, and vice versa, are represented.

As a first step, a preliminary estimation of the power losses is conducted using the RT electro-thermal model. This model must consider the driving profiles of the vehicle, together with the controller, power electronics and electric machine model to estimate such losses under realistic driving conditions. As the virtual junction temperature of the devices $T_{v,j}$ has a significant influence on the instantaneous transistor ($P_{loss,M}$) and diode ($P_{loss,D}$) power losses, its influence must be modelled to achieve sufficiently accurate results. In this step, the 1D equivalent network is not yet available; thus, constant nominal temperatures are considered as a first approximation. Once the power loss profiles of all semiconductors during the whole driving cycle have been obtained, the average power loss distribution between the elements is determined ($\%_{loss}$). Thanks to this, adequate power steps are defined as inputs for the 3D FEM heat source characterization stage. From the thermal response results ($T_{die,M}$, $T_{die,D}$) of such power loss steps obtained by FEM, the equivalent thermal impedances of the power semiconductors are extracted by their post-processing. Being this point of particular importance for the accuracy of the results, the post-processing procedure is thoroughly explained in section 4. Once the equivalent Foster networks (RC_M, RC_D) are calculated, they are implemented in the 1D RT model and the power loss profiles (P_M, P_D) are re-calculated, also obtaining the temperature profiles (T_M, T_D) corresponding to the $T_{v,j}$ of all the semiconductors (and the ones corresponding to the intermediate points that are represented by the simplified 1D Foster network).

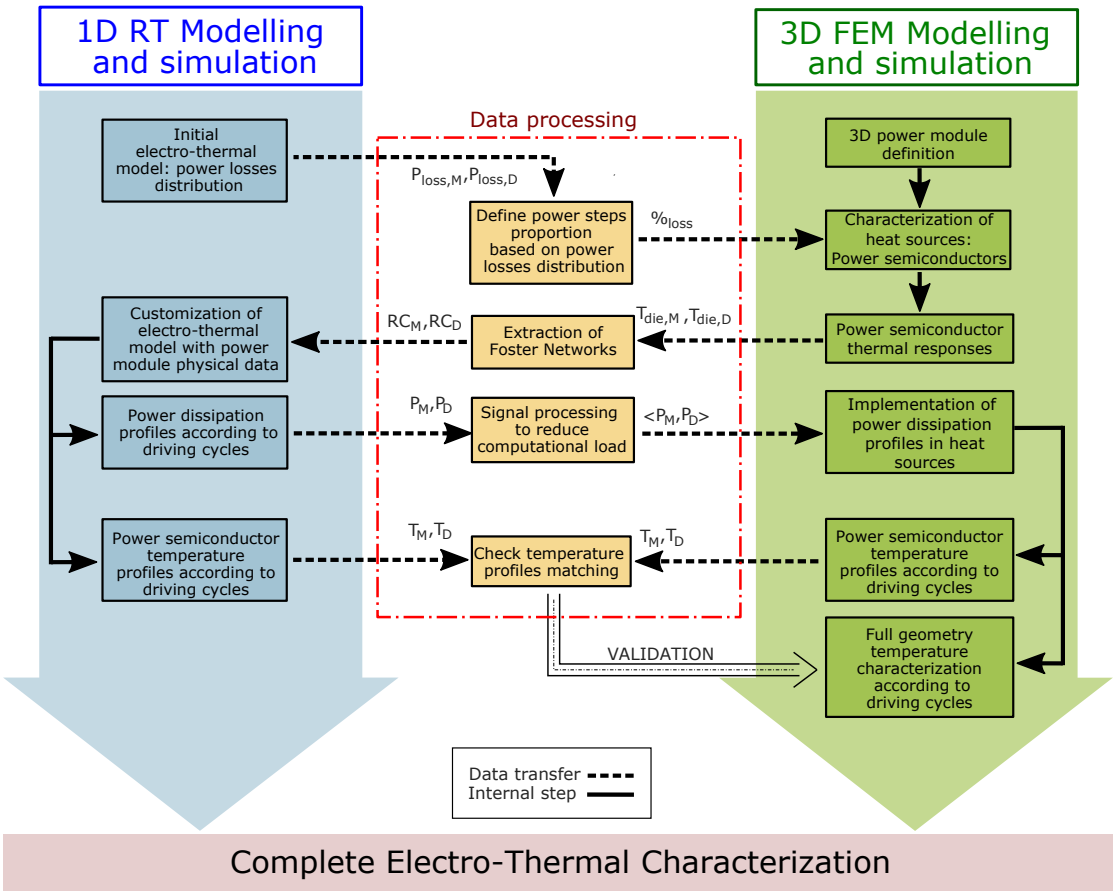

Figure 1: General diagram of the proposed methodology to characterize the electro-thermal behaviour of an automotive power module through driving cycles.

In the following step, the power dissipation profiles are averaged ($< P_M, P_D >$) (by post-processing), and they are introduced for the complete driving cycle simulation in the FEM model, significantly reducing the required computational burden. As a result, a complete figure of the power module thermal distribution through the driving cycle is obtained, which allows the detection of hot points and incorrect thermal distributions through the designed layout. This information will be used to detect reliability problems and support the design process of the module.

As a final step, the matching between the temperature profiles (T_M, T_D) obtained by means of the 1D and 3D methods over the driving cycles is carried out, as this can be used to confirm the correct characterization of the heat sources and power module. The details of the 1D RT and 3D FEM modelling and simulation are explained in sections 3 and 4, respectively.

3. Real-time 1D electro-thermal simulation platform

In order to accurately determine the power losses and power semiconductor junction temperatures over standardized driving cycles, a complete EV propulsion system model is required, including a vehicular model, digital controller, power electronics model (with the corresponding loss and 1D thermal models per device) and electric machine model. Details regarding such implementation can be found in [9]. Considering the duration of the driving cycles and the complexity and computational load of such model, conventional simulation procedures become almost infeasible. However, the usage of high performance real-time digital simulation can overcome such problems.

In this work, an RT-Lab OP4510 digital real-time simulation platform [31] consisting on four CPUs (3.5 GHz) and a Xilinx Kintex7 FPGA has been used to conduct the real-time simulations. The elements that constitute the model have been distributed as shown in Figure 2(a) between the computational nodes available in the OP4510 device. The vehicular digital controller (Figure 2(a) ①) and 1D thermal and loss models (including temperature dependency) have the slowest time-constants (Figure 2(a) ②); thus, such models have been distributed between the two available CPUs for their computation in parallel. On the other hand, the power converter and the electric machine models with short simulation step requirements have been implemented in the FPGA ((Figure 2(a) ③)) using the eHS solver [32]. In this way, real-time execution has been guaranteed, greatly reducing the time required to perform such simulations.

4. Equivalent RC network extraction procedure

The equivalent thermal network extraction is capital to obtain accurate results. This requires a number of steps, as shown in

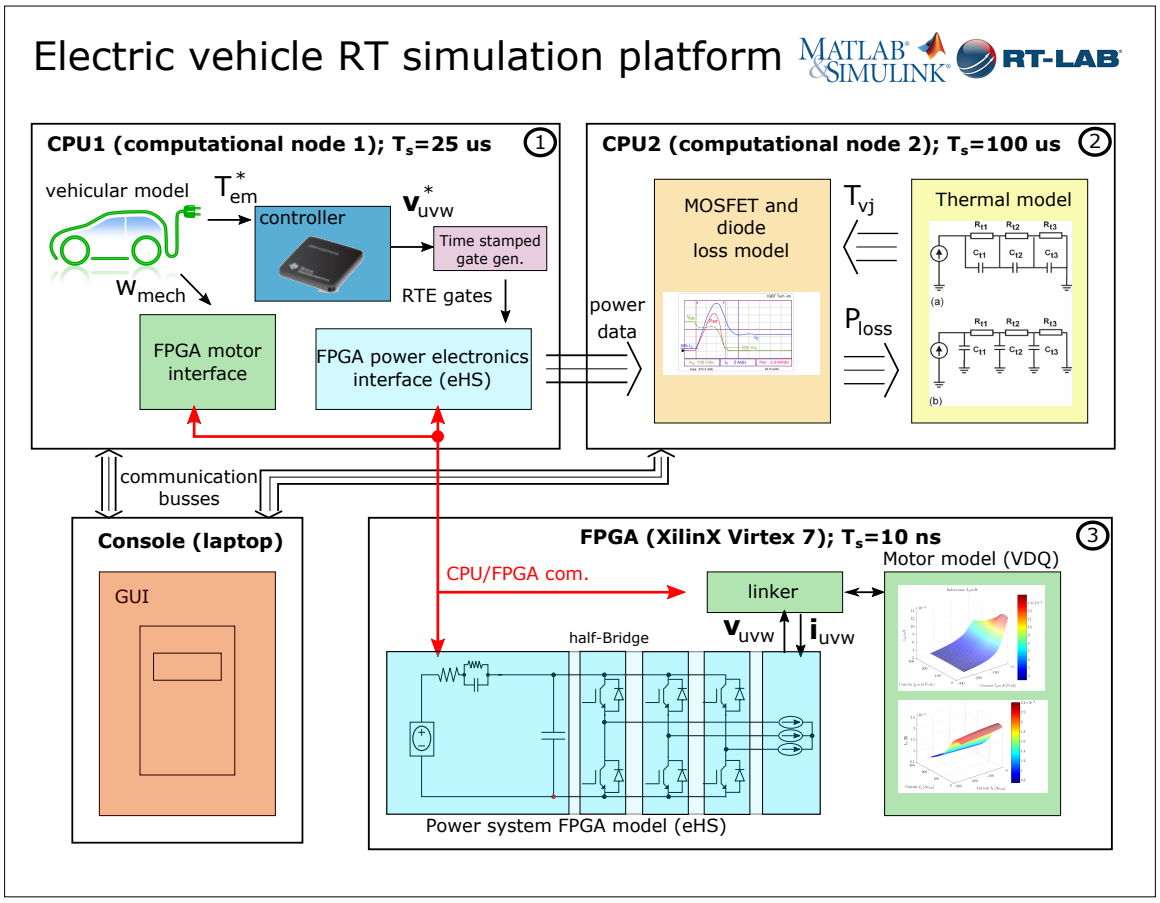

(a) General diagram of the 1D RT EV propulsion system model based on FPGA and CPU cosimulation.

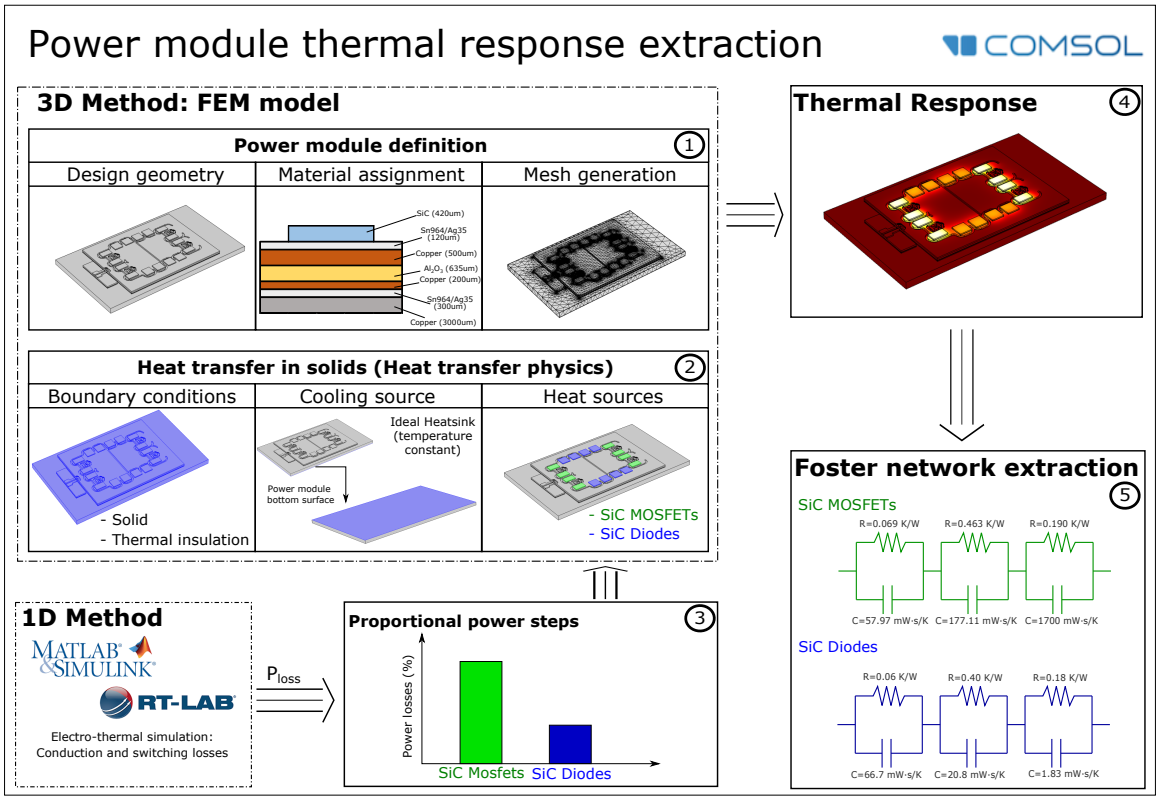

(b) General diagram of the 3D FEM simulation work-flow for thermal network extraction.

Figure 2: General diagrams of the 1D RT and 3D FEM simulations.

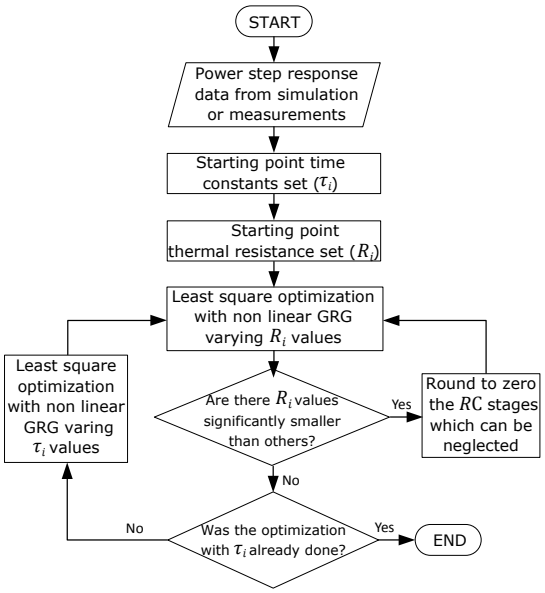

Figure 3: Flowchart of the procedure applied to extract the Foster networks.

Figure 2(b). As a starting point, the power module must be represented in 3D (Figure 2(b) ①), implementing the layout geometry, the layer material assignment (taking into account the surface contact characteristics) and the mesh generation (determining the number of elements) [18]. Additionally, the input signals for the characterization must be defined, so that boundary conditions, cooling and heat sources have to be implemented (Figure 2(b) ②). After that, the preliminary weighted power dissipation steps obtained by real-time simulation (Figure 2(b) ③) must be applied over the heat sources, and the transient responses (Figure 2(b) ④) must be analysed to extract the equivalent 1D Foster networks (Figure 2(b) ⑤). In this context, the power device time-dependant thermal impedance $Z_{j-c}(t)$ can be expressed by a finite sum of exponential terms [33]:

$$Z_{j-c}(t) = \sum_{i=1}^{n} R_i \left(1 - e^{-\frac{t}{\tau_i}}\right), \tag{1}$$

where R_i and τ_i are the thermal resistance and the time constant of the i-th stage of the thermal network. The time constant is given by $\tau_i = R_i \cdot C_i$, where C_i is the thermal capacitance of the i-th stage. Typically, the thermal impedance can be well fitted considering an equivalent thermal network composed by 3 to 5 stages [34].

The Foster network R_i and C_i couples can be evaluated by using a variety of methods, such as the perturb and observe approach combined with a least square minimization [35], the Levenberg-Marquardt nonlinear fit-routine [36], the identification by deconvolution [33], and the particle swarm optimization [37]. However, in this particular case, the procedure described in [38] and depicted in Figure 3 has been selected, where the degrees of freedom are reduced by choosing a logarithmically-spaced set of time constants (τ_i) in a reasonable interval. The procedure can be automated with a Matlab or Python script in order to reduce the computational load. The steps of the recursive procedure are the following:

Table 2: Main parameters of the simulated system for SiC half-bridge electro-thermal characterization.

Parameter	Symbol	Value	Units
Vehicle model parameters			
Vehicle total mass	M_{car}	1030	kg
Rotating mass	M_{rot}	5	%
Vehicle cross section	A_f	2.42	m^2
Wheel radius	r_{wheel}	0.29	m
Gravity acceleration	a_g	9.81	m/s^2
Rolling friction coefficient	μ	0.008	-
Air density	ρ	1.225	kg/m^3
Drag coefficient	C_d	0.367	-
Transmission model parameters			
Gear ratio	GR	6.2	-
Efficiency	η_{GR}	97	%
Idling losses	P_{Idling}	300	W
Electric machine parameters: AF130			
Maximum speed	ω_{max}	8000	rpm
Nominal torque	T_N	145	Nm
Peak torque (20 s)	T_p	350	Nm
Nominal power	P_N	64	kW
Peak power (20 s)	P_p	140	kW
Power converter nominal parameters			
DC link capacitance	C_{DC}	700	μF
Switching frequency	f_{SW}	10	kHz
Battery voltage	V_{batt}	360	V
Gate resistance (ON/OFF)	R_G	5	Ω
SiC MOSFET parameters: CPM2-1700-0045B (Cree)			
Nominal current per switch	$I_{D,nom}$	48	A
Maximum blocking voltage	$V_{DS,max}$	1700	V
Operating junction temperature	T_{vj}	-40 to +150	^oC
SiC diode parameters: CPW5-1700-Z050B (Cree)			
Maximum current per switch	$I_{F,max}$	50	A
Repetitive peak reverse voltage	V_{RRM}	1700	V
Typical DC forward voltage	V_F	1.6	V
Operating junction temperature	T_{vj}	-55 to +175	^oC

1. Set as input data the simulated (or measured) time dependant thermal impedance between the points of interest and the reference temperature, applying a power step to the module devices.

2. Choose a number (e.g. 10 or more) of logarithmically spaced time constants τ between a very small instant (e.g. 1 ps or 1 ns) and an instant when the transient can be considered terminated (steady state reached).

3. Set positive reasonable values (e.g. values whose sum gives a fitting steady state temperature near the one obtained by simulations) of R_i as a starting point for the next optimization step.

4. Use the R_i set as variable for a least square minimization using the Generalized Reduced Gradient (GRG) method [39] in a non-linear optimization tool (e.g. in Matlab).

5. Decimate the time constants, erasing those with the smaller thermal resistances obtained at step 3. At this step,

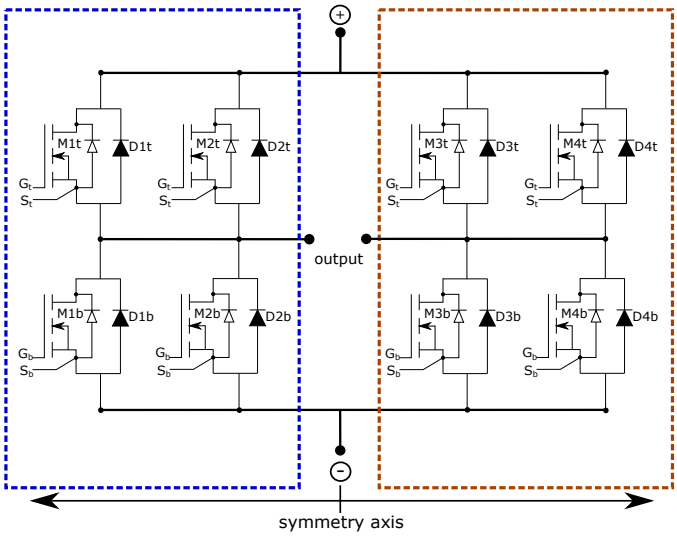

Figure 4: SiC half-bridge with four SiC MOSFETs and SiC diodes in parallel incorporating a symmetrical design.

the non-zero time constants, which do not change significantly the sum of squared residuals (obtained as result of optimization step), are neglected.

6. Introduce the decimated τ_i set as variable for a least square minimization using the GRG method in a non-linear optimization tool.

7. Run step 4 again.

Once the most relevant aspects of the proposed methodology have been presented, an application example is provided, where a SiC half-bridge is electro-thermally simulated following the proposal.

5. Results obtained from the application of the proposed methodology for an automotive SiC half-bridge module

With the aim of applying the proposed methodology and demonstrate its effectiveness, a hybrid electro-thermal simulation of an automotive power converter has been carried out. The converter of the simulated EV propulsion system is a two-level three-phase Voltage Source Inverter (VSI) that feeds a 64 kW automotive axial flux Surface Mounted Permanent Magnet Synchronous Machine (SM-PMSM). This inverter consists of three SiC half-bridge modules, each one composed by four paralleled SiC MOSFETs and SiC diodes per level (Figure 4). The electro-thermal data has been extracted from the SiC half-bridge layout, which is the unit to be studied in this example.

Regarding the vehicle, a baseline A segment EV has been implemented in the model. The most significant mechanical parameters of the vehicle and the electrical and mechanical parameters of its particular propulsion system are shown in Table 2. A driving cycle specifically created for EV driving characterization, named Flet-BEV-cycle, has been applied [40]. Such speed-versus-time driving profile has been processed considering the vehicular model in order to determine the instantaneous electric machine electromagnetic torque T_{em} (Figure 5(a)) and mechanical speed ω_{mech} (Figure 5(b)).

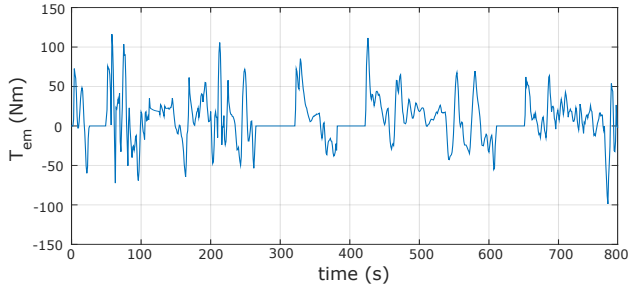

(a) Torque profile obtained when applying the Fleet-BEV driving cycle.

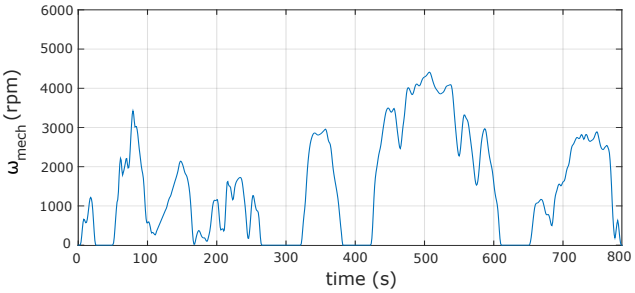

(b) Speed profile obtained when applying the Fleet-BEV driving cycle.

Figure 5: Torque and speed profiles applied during the simulations.

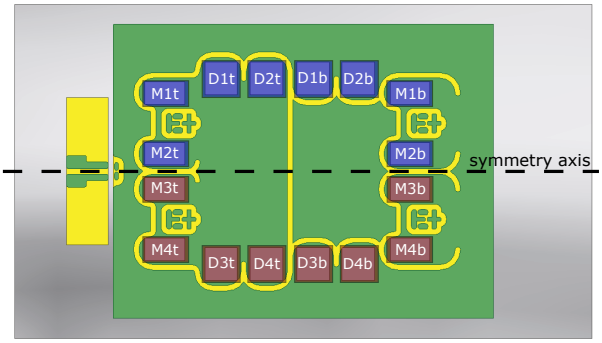

(a) Top view of power module layout, showing the symmetry.

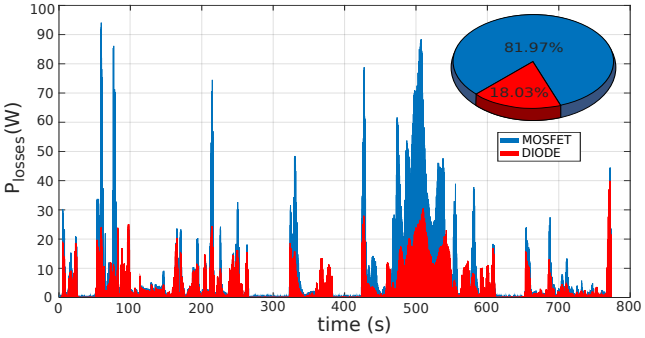

(b) Initial power losses distribution between SiC MOSFETs and diodes.

Figure 6: Power layout and power losses distribution.

5.1. Definition of power layout and initial approximation

In addition to the propulsion system set-up, the layout of the power module also has to be defined. The geometry, the materials and the power semiconductors (heat sources) are the fundamental elements to be specified in the 3D model for the extraction of accurate Foster networks. For this case study, the SiC half-bridge layout shown in Figure 6(a), which incorporates a symmetrical design, has been implemented. Such symmetry re-

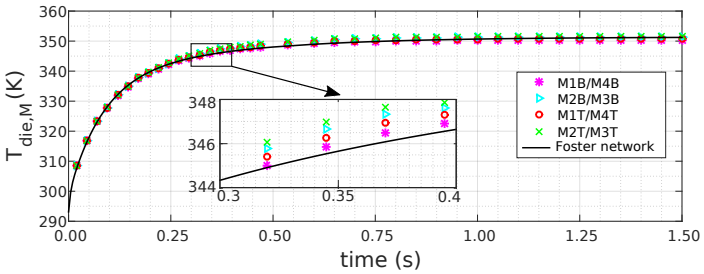

(a) Power step temperature response of the SiC MOSFET.

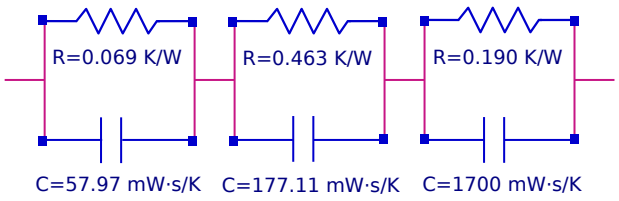

(b) Equivalent Foster network of SiC MOSFETs.

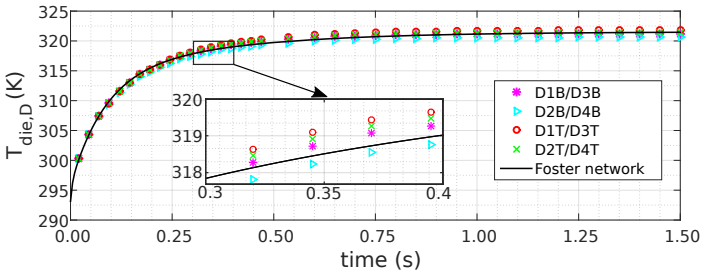

(c) Power step temperature response of the SiC diode.

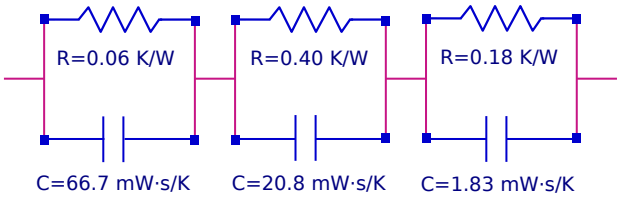

(d) Equivalent Foster network of SiC diodes.

Figure 7: Thermal responses and equivalent Foster networks.

duces the amount of Foster networks to be determined, because devices in symmetric positions will show equivalent thermal behaviours, as indicated in the following:

$$\begin{aligned} &M1t \equiv M4t;\ M2t \equiv M3t; M1b \equiv M4b;\ M2b \equiv M3b; \\ &D1t \equiv D3t;\ D2t \equiv D4t; D1b \equiv D3b;\ D2b \equiv D4b, \end{aligned} \tag{2}$$

where Mit and Mib represent the top and bottom SiC MOSFETs, respectively, and Dit and Dib represent the top and bottom SiC diodes, respectively, being $i = \{1...4\}$.

As detailed in section 2, a preliminary estimation of power losses is required prior equivalent Foster network extraction. In this context, the power loss distribution shown in Figure 6(b) has been obtained for this particular case study.

5.2. *Determination of the equivalent Foster networks*

The power semiconductors are the points of interest to extract the equivalent Foster networks, as they are the heat sources of the power module. In order to obtain the RC networks of the SiC half-bridge, a power step (proportional to the previously determined power loss distribution) has been applied to each semiconductor in the 3D FEM model. As a result, the thermal transient responses of the devices have been obtained (Figures 7(a) and 7(c)).

These results verify the layout symmetry (2). In addition and according to these results, the Foster representation of the devices can be simplified using a unique Foster representation for all the SiC MOSFETs of the half-bridge, and another unique representation for all SiC diodes:

$$\begin{aligned} &M1t \equiv M2t \equiv M3t \equiv M4t \equiv M1b \equiv M2b \equiv M3b \equiv M4b; \\ &D1t \equiv D2t \equiv D3t \equiv D4t \equiv D1b \equiv D2b \equiv D3b \equiv D4b. \end{aligned} \tag{3}$$

Finally, applying the RC network extraction procedure described in section 4, an equivalent 3 stages Foster network has been calculated for SiC MOSFETs (Figures 7(b)) and SiC diodes (Figure 7(d)). The relative error of these RC networks is lower than 2%. Then, a quite good matching between the thermal responses and the fitted Foster network curves (Figures 7(a) and 7(c)) has been obtained.

5.3. *Determination of power dissipation profiles by means of real-time simulation*

The power dissipation profiles of the semiconductors have been later calculated using the 1D RT simulation platform, by introducing the equivalent Foster network extracted from the 3D FEM. Such power dissipation profiles for a Fleet-BEV-cycle are shown in Figure 8, where no significant differences between paralleled devices are found, as they are thermally modeled by the same equal Foster networks.

After obtaining such profiles, they have been imported into the 3D FEM in order to characterize the physical heat sources during the complete driving cycle. As the FEM simulation has a much higher computational burden than a 1D model, an adequate averaging of the simulation inputs (power loss profiles) is fundamental to reduce the number of computed samples over the time without losing accuracy. The 1D RT simulation calculates power loss data with a high resolution (sampling time of 100 μs). Such data has been averaged applying a moving mean over a period of 50 ms.

5.4. *Power module 3D temperature characterization over the entire driving cycle*

Considering the high computational resources requested by of FEM transient simulations, simplifications based on the symmetry of the layout can be applied to significantly reduce the workload. In this case and considering the symmetry of the SiC half-bridge, it is possible to reduce the number of elements to be evaluated. For this reason, only one half of the power module

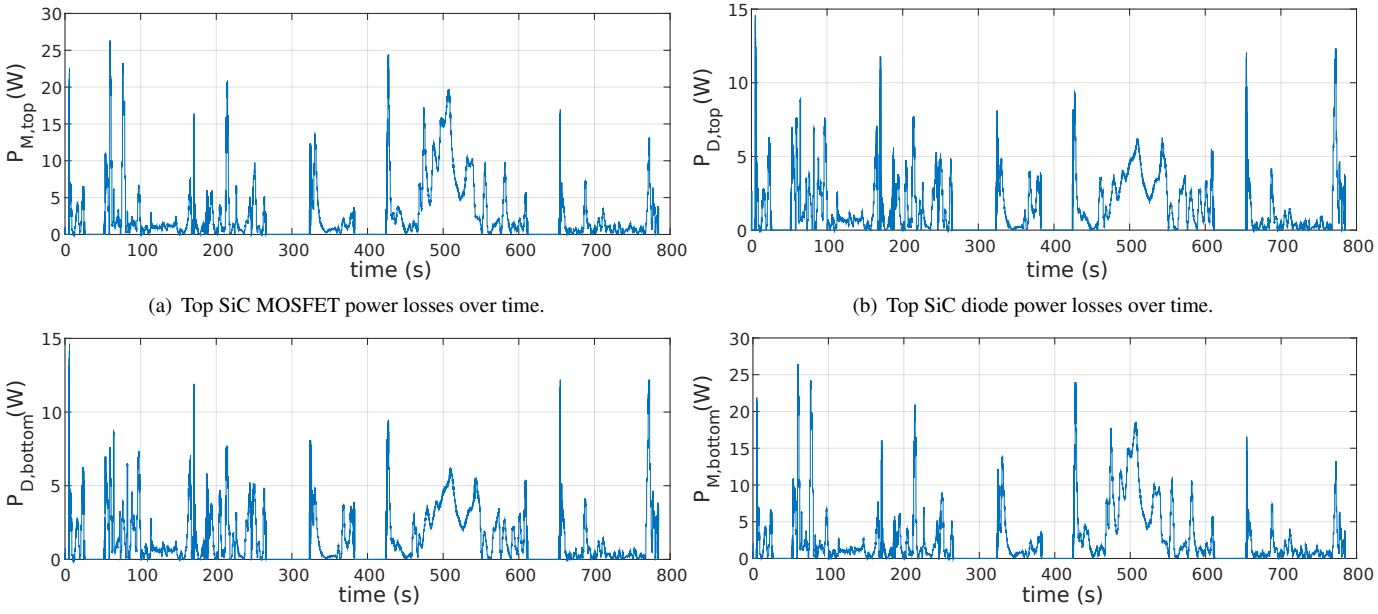

(a) Top SiC MOSFET power losses over time.

(b) Top SiC diode power losses over time.

(c) Bottom SiC MOSFET power losses over time.

(d) Bottom SiC diode power losses over time.

Figure 8: Power dissipation profiles of power semiconductors: heat sources of the electro-thermal model.

needs to be simulated (using the symmetry axis, figure 6(a)), extrapolating the result to the other half.

From the application of the previously calculated power loss profiles over the 3D model, Figures 9(a)-9(d) show the thermal distribution of the half-bridge power module in four relevant operation points during the application of the Fleet-BEV driving cycle. Such results show that the power module has a good thermal distribution without significant asymmetries or excessive hot points.

As a final step and in order to validate the obtained results, the instantaneous temperature profiles calculated at each semiconductor junction by means of 1D and 3D simulation have been compared. A good matching between the temperature variations obtained by both methods can be observed in Figures 9(e)-9(h).

6. Conclusions

Considering the results obtained in this work, the proposed hybrid methodology can be considered as an useful tool for the thermal characterization of power automotive power converters, and also for the detection of reliability problems and design errors. The following benefits can be concluded:

1. The usage of a unique physical domain (thermal) in the 3D FEM reduces the computational burden and the number of convergence problems, being it feasible to simulate long EV driving profiles with a duration of hundreds of seconds.

2. Accurate equivalent RC networks can be obtained according to the specific layout and layer materials. This is of great interest when studying novel power modules under design, or also when analysing commercial power modules where no thermal data are provided.

3. The usage of a 1D RT platform significantly reduces the required time to carry out simulation without any significant accuracy loss.

4. The matching between the semiconductor temperature profiles obtained by 1D RT and 3D FEM simulations guarantees the confidence on the obtained results.

5. Critical differences between thermal impedances between the semiconductors can be detected through the power devices thermal responses. Thus, correction actions to get more reliable systems can be taken since the early design stages, reducing development time and costs.

6. In the 3D thermal characterization, the application of some simplifications is possible considering the particular geometry without a loss of accuracy, further reducing the required computational time.

7. Acknowledgements

This work has been supported by the Department of Education, Linguistic Policy and Culture of the Basque Government within the fund for research groups of the Basque university system IT978-16, by the Government of the Basque Country within the research program ELKARTEK as the project ENSOL (KK-2018/00040), and by the program to support the education of researches of the Basque Country *PRE*_2017_2_0008.

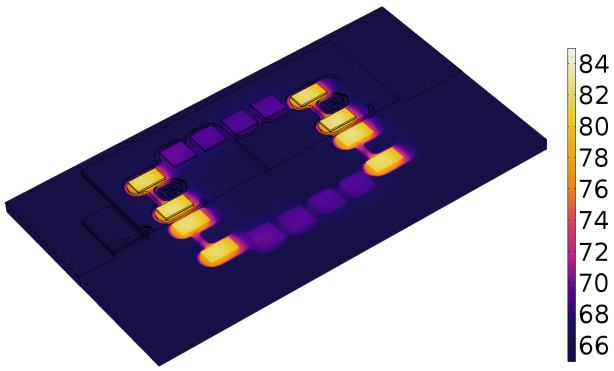

(a) 3D Temperature distribution (°C) of the module at t = 60 *s*.

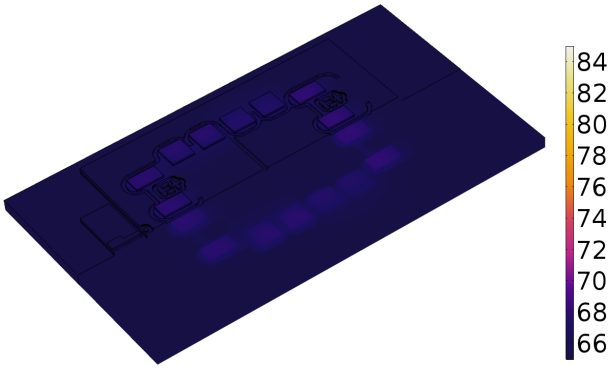

(b) 3D Temperature distribution (°C) of the module at t = 244.8 *s*.

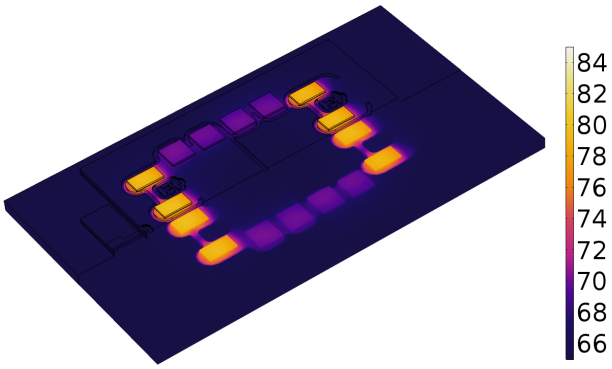

(c) 3D Temperature distribution (°C) of the module at t = 428 *s*.

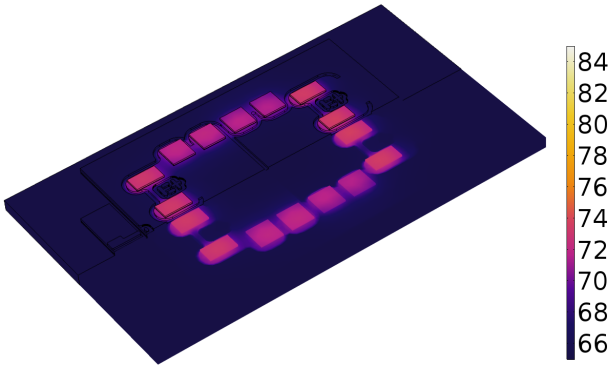

(d) 3D Temperature distribution (°C) of the module at t = 773 *s*.

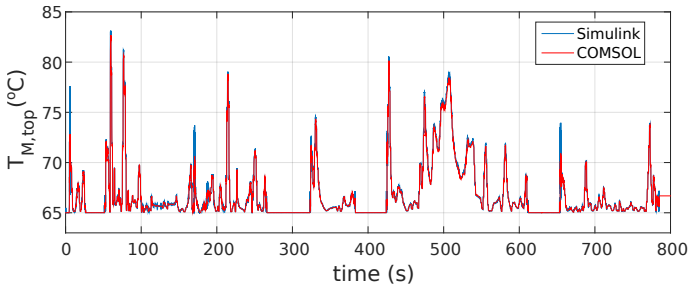

(e) Top SiC MOSFET temperature profiles.

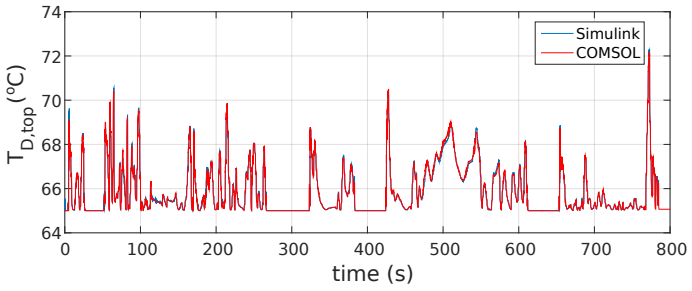

(f) Top SiC diode temperature profiles.

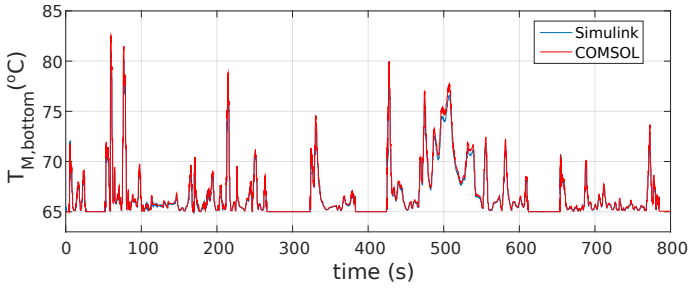

(g) Bottom SiC MOSFET temperature profiles.

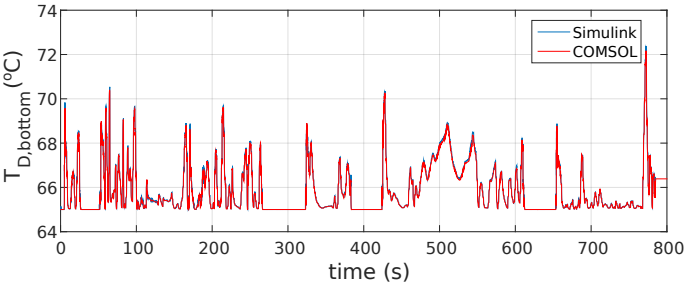

(h) Bottom SiC diode temperature profiles.

Figure 9: 3D thermal results obtained on the power module and junction temperature profiles of power semiconductors during the complete driving cycle .

References

[1] Global EV outlook 2018: Towards cross-modal electrification, Tech. rep., International Energy Agency (2018).

[2] S. Rastogi, A. Sankar, K. Manglik, S. Mishra, S. Mohanty, Toward the Vision of All-Electric Vehicles in a Decade (Energy and Security), IEEE Consumer Electronics Magazine 8 (2) (2019) 103–107 (2019).

[3] C. Capasso, O. Veneri, Experimental analysis on the performance of lithium based batteries for road full electric and hybrid vehicles, Applied Energy 136 (2014) 921–930 (2014).

[4] K. T. Chau, W. Li, Overview of electric machines for electric and hybrid vehicles, International Journal of Vehicle Design 64 (1) (2014) 46–71 (2014).

[5] J. Riba, C. Lomonova, E. Lopez, L. Romeral, A. Garcia, Rare-earth-free propulsion motors for electric vehicles: A technology review, Renewable and Sustainable Energy Reviews 57 (2016) 367–379 (2016).

[6] A. Stefanskyi, L. Starzak, A. Napieralski, Silicon carbide power electronics for electric vehicles, in: Proc. of the International Conference on Ecological Vehicles and Renewable Energies (EVER), 2015 (2015).

[7] J. Reimers, L. Dorn-Gomba, C. Mak, A. Emadi, Automotive Traction Inverters: Current Status and Future Trends, IEEE Transactions on Vehicular Technology 68 (4) (2019) 3337–3350 (2019).

[8] B. Wu, D. Kim, B. Han, A. Palczynska, A. Prisacaru, P. Gromala, Hybrid Approach to Conduct Failure Prognostics of Automotive Electronic Control Unit Using Stress Sensor as In Situ Load Counter, IEEE Transactions on Components, Packaging and Manufacturing Technology 9 (1) (2019) 28–38 (2019).

[9] E. Trancho, E. Ibarra, A. Arias, I. Kortabarria, P. Prieto, I. Martinez de Alegria, J. Andreu, I. Lopez, Sensorless control strategy for light-duty EVs and efficiency loss evaluation of high frequency injection under standardized urban driving cycles, Applied Energy 224 (2018) 647–658 (2018).

[10] S. Waye, High temperature air-cooled power electronics thermal design, Tech. rep., National Renewable Energy Laboratory (2016).

[11] I. Aranzabal, I. Martinez de Alegria, N. Delmonte, P. Cova, I. Kortabarria, Comparison of the heat transfer capabilities of conventional single-phase and two-phase cooling systems for electric vehicle IGBT power module, IEEE Transactions on Power Electronics-doi:10.1109/TPEL.2018.2862943.

[12] T. Ogawa, A. Tanida, T. Yamakawa, M. Okamura, Verification of fuel efficiency improvement by application of highly effective silicon carbide power semiconductor to HV inverter, in: Proc. of the SAE World Congress and Exhibition, 2016, pp. 1–5 (2016).

[13] X. Ding, M. Du, T. Zhou, H. Guo, C. Zhang, Comprehensive comparison between silicon carbide MOSFETs and silicon IGBTs based traction systems for electric vehicles, Applied Energy 194 (2016) 626–634 (2016).

[14] A. Christmann, Silicon carbide (SiC) semiconductors for xEV are getting closer to reality, in: Proc. of the SAE Hybrid Symposium, 2018 (2018).

[15] C. Qian, A. Gheitaghy, J. Fan, H. Tang, B. Sun, H. Ye, G. Zhang, Thermal management on IGBT power electronic devices and modules, IEEE Access 6 (2018) 12868–12884 (2018).

[16] A. Soldati, G. Pietrini, M. Dalboni, C. Concari, Electric-vehicle power converters model-based design-for-reliability, CPSS Transactions on Power Electronics and Applications 3 (2) (2018) 102–110 (2018).

[17] P. Reigosa, H. Wang, Y. Yang, F. Blaabjerg, Prediction of bond wire fatigue of IGBTs in a PV inverter under a long-term operation, IEEE Transactions on Power Electronics 31 (10) (2016) 7171–7182 (2016).

[18] H. Chen, J. Yang, S. Xu, Electro-thermal Based Junction Temperature Estimation Model for Power Converter of Switched Reluctance Motor Drive System, IEEE Transactions on Industrial Electronics (2019). doi:10.1109/TIE.2019.2898600.

[19] J. Li, A. Castellazzi, M. Eleffendi, E. Gurpinar, C. Johnson, L. Mills, A physical RC network model for electrothermal analysis of a multichip SiC power module, IEEE Transactions on Power Electronics 33 (3) (2018) 2494–2508 (2018).

[20] M. Ouhab, Z. Khatir, A. Ibrahim, J. Ousten, R. Mitova, M. Wang, New analytical model for real-time junction temperature estimation of multichip power module used in a motor drive, IEEE Transactions on Power Electronics 33 (6) (2018) 5292–5301 (2018).

[21] C. van der Broek, L. Ruppert, M. Conrad, R. De Doncker, Spatial electrothermal modeling and simulation of power electronic modules, IEEE Transactions on Industry Applications 54 (4) (2018) 404–415 (2018).

[22] J. Ko, D. Jin, W. Jang, C. Myung, S. Kwon, S. Park, Comparative investigation of NOx emission characteristics from a Euro 6-compliant diesel passenger car over the NEDC and WLTC at various ambient temperatures, Applied Energy 187 (2017) 652–662 (2017).

[23] L. Chen, J. Wang, P. Lazari, X. Chen, Optimizations of a Permanent Magnet Machine Targeting Different Driving Cycles for Electric Vehicles, in: Proc. of the IEEE International Electric Machines & Drives Conference (IEMDC), 2013, pp. 855–862 (2013).

[24] M. Rasid, A. Ospina, K. Benkara, V. Lanfranchi, A thermal study on small synchronous reluctance machine in automotive cycle, in: Proc. of the IEEE International Symposium on Industrial Electronics (ISIE), 2016, pp. 134–140 (2016).

[25] G. Pasaoglu, D. Fiorello, A. Martino, L. Zani, A. Zubaryeva, C. Thiel, Travel patterns and the potential use of electric cars - results from a direct survey in six european countries, Technological Forecasting & Social Change 87 (2014) 51–59 (2014).

[26] A. Bahman, K. Ma, P. Ghimire, F. Iannuzzo, F. Blaabjerg, A 3-D lumped thermal network model for long-term load profiles analysis in high-power IGBT modules, IEEE Journal of Emerging and Selected Topics in Power Electronics 4 (3) (2016) 1050–1063 (2016).

[27] B. Gao, F. Yang, M. Chen, L. Ran, I. Ullah, S. Xu, P. Mawby, A temperature gradient-based potential defects identification method for IGBT module, IEEE Transactions on Power Electronics 32 (3) (2017) 2227–2242 (2017).

[28] A. Raciti, D. Cristaldi, G. Greco, G. Vinci, G. Bazzano, Electrothermal PSpice Modeling and Simulation of Power Modules, IEEE Transactions on Industrial Electronics 62 (10) (2015) 6260–6271 (2015).

[29] J. Ye, K. Yang, H. Ye, A. Emadi, A Fast Electro-Thermal Model of Traction Inverters for Electrified Vehicles, IEEE Transactions on Power Electronics 32 (5) (2017) 3920–3934 (2017).

[30] L. Ceccarelli, R. M. Kotecha, A. S. Bahman, F. Iannuzzo, A. H. Mantooth, Mission-profile-based lifetime prediction for a SiC MOSFET power module using a multi-step condition-mapping simulation strategy, IEEE Transactions on Power Electronics (2019). doi:10.1109/TPEL.2019.2893636.

[31] H. Chen, C. Gan, B. Xia, P. Rafajdus, RT-LAB simulator platform for simulation of switched reluctance machine, in: Proc. of the IEEE International Symposium on Industrial Electronics (ISIE), 2012, pp. 737–741 (2012).

[32] J. Belanjer, A. Yamane, A. Yen, S. Cense, P. Robert, Validation of eHS FPGA reconfigurable low-latency electric and power electronic circuit solver, in: Proc. of the IEEE Industrial Electronics Society Conference (IECON), 2013, pp. 5418–5423 (2013).

[33] V. Székely, A new evaluation method of thermal transient measurement results, Microelectronics Journal 28 (3) (1997) 277 – 292, thermal Investigations of ICs and Microstructures (1997).

[34] A. Hensler, C. Herold, J. Lutz, M. Thoben, Thermal impedance monitoring during power cycling tests, in: Proc. of the Int. Exhib. Conf. Power Convers., Intell. Motion Power Quality, 2011, pp. 241–246 (2011).

[35] D. Chiozzi, M. Bernardoni, N. Delmonte, P. Cova, A simple 1-D finite elements approach to model the effect of PCB in electronic assemblies, Microelectronics Reliability 58 (2016) 126–132 (2016).

[36] Y. Gerstenmaier, W. Kiffe, G. Wachutka, Combination of thermal subsystems modelled by rapid circuit transformation, in: Proc. of the International Workshop on Thermal Investigation of ICs and Systems (THERMINIC), 2008, pp. 115–120 (2008).

[37] O. Alavi, M. Abdollah, A. H. Viki, Assessment of thermal network models for estimating IGBT junction temperature of a buck converter, in: Proc. of the Power Electronics, Drive Systems & Technologies Conference (PEDSTC), 2017, pp. 102–107 (2017).

[38] M. Bernardoni, N. Delmonte, D. Chiozzi, P. Cova, Non-linear thermal simulation at system level: Compact modelling and experimental validation, Microelectronics Reliability 80 (2018) 223–229 (2018).

[39] L. S. Lasdon, R. L. Fox, M. W. Ratner, Nonlinear optimization using the generalized reduced gradient method, RAIRO-Operations Research-Recherche Opérationnelle 8 (3) (1974) 73–103 (1974).

[40] M. Pfriem, F. Gauterin, Development of real-world driving cycles for battery electric vehicles, in: Proc. of the EVS29 International Battery, Hybrid and Fuel Cell Electric Vehicle Symposium, 2016, pp. 1–11 (2016).